17th International Conference on Greenhouse Gas Control Technologies, GHGT-17

20th -24th October 2024 Calgary, Canada

Reservoir simulations and accuracy measures for CO_2 and pressure plumes for the Broom Creek Formation in central North Dakota

Kyoung Min*, Matthew E. Burton-Kelly, Gabriela A. Martinez, Alexander Chakhmakhchev, Matthew L. Belobraydic, Nicholas A. Azzolina, and Wesley D. Peck

Energy & Environmental Research Center, University of North Dakota, 15 North 23rd Street, Stop 9018, Grand Forks, ND, USA

Abstract

This study estimated the accuracy of the predicted 5-year carbon dioxide (CO_2) and pressure plumes for a hypothetical geological storage project injecting CO_2 into the Broom Creek Formation near central North Dakota. A detailed, fine-scaled geomodel, defined as the standard reference geomodel (SRG), was developed to represent the lithofacies and petrophysical properties observed in the Broom Creek Formation near central North Dakota. Three derivative geomodels (DGs) were generated by sampling five wells within the SRG. Synthetic logs acquired from these five wells were used to create one base-case DG (DG-Base) and two permutations of the base case developed with shorter (DG-Short) and longer (DG-Long) variogram lengths. An industry-standard workflow was deployed to develop these three DGs, thereby producing models that are representative of those that would be generated from real-world data for commercial storage projects (i.e., geomodels derived from the SRG). Reservoir simulations of CO_2 injection were done in the SRG, DG-Base, DG-Short, and DG-Long geomodels. The 5-year simulated CO_2 and pressure plumes in the storage unit were compared between the SRG and the three derivative models using different measures to quantify accuracy, where the SRG-simulated results were defined as the true outcome. A novel application of similarity metrics within a 2D grid was used to assess the accuracy between the SRG and DG simulations. Despite the sources of uncertainty in the geomodels and reservoir simulations, the comparative assessments showed that the DG simulations could predict the 5-year CO_2 plume at a storage site to within 200–800 meters. Additional testing could assess these accuracies more definitively and validate these preliminary findings.

Keywords: carbon capture and sequestration; geological modeling; reservoir simulation; similarity metrics; accuracy

1. Introduction

Two major elements of Class VI permitting requirements for carbon dioxide (CO_2) geological storage projects (storage projects) are the predicted CO_2 and pressure plumes in the storage unit in response to CO_2 injection. These predictions are generated through a three-step process that includes 1) site characterization activities that acquire site-specific geological and petrophysical data, 2) the construction of a site-specific geomodel of the storage unit and primary confining layer(s) using the site characterization data, and 3) reservoir simulations of CO_2 injection into the storage unit within the geomodel. The results of the reservoir simulations are used to predict the CO_2 and pressure buildup plumes throughout the injection and postinjection periods and are an integral part of the permit documents; they also inform the development of risk management and monitoring plans. Unlike reservoir simulations for oil and

* Corresponding author. Email address: kmin@undeerc.org

gas reservoirs, which often have monthly oil, gas, and water production data to history-match (calibrate) the geomodel and simulations, storage projects in deep saline formations typically will not have data on the location and extent of the CO_2 and pressure plumes for 1–5 years after the start of injection. Consequently, the permitting process for storage projects heavily relies on site characterization data (the geomodel) and forward modeling (prediction with reservoir simulation), especially during the early years of the injection period.

This work estimates the accuracy of the predicted 5-year CO_2 and pressure plumes for a hypothetical storage project that injects CO_2 into the Broom Creek Formation near central North Dakota. In western and central North Dakota, the Broom Creek Formation is an excellent candidate for the geological storage of CO_2 [1, 2]. Several storage projects targeting the Broom Creek Formation have been permitted in North Dakota [3], and multiple future projects targeting the Broom Creek Formation are planned. A detailed, fine-scaled geomodel, defined as the standard reference geomodel (SRG), was developed to represent the lithofacies and petrophysical properties observed in the Broom Creek Formation near central North Dakota. Three derivative geomodels (DGs) were generated by sampling five wells within the SRG. Synthetic logs acquired from these five wells were used to create one base-case DG (DG-Base) and two permutations of the base case developed with shorter (DG-Short) and longer (DG-Long) variogram lengths. An industry-standard workflow was deployed to develop these three DGs, thereby producing models that are representative of those that would be generated from real-world data for commercial storage projects (i.e., geomodels derived from the SRG). Reservoir simulations of CO_2 injection were done in the SRG, DG-Base, DG-Short, and DG-Long geomodels. The 5-year simulated CO_2 and pressure plumes in the storage unit were compared between the SRG and the three derivative models. Different measures were used to quantify accuracy, where the SRG-simulated results were defined as the true outcome. A comparison of these SRG and DG simulation results was used to evaluate the ability of the DGs to predict the performance of the storage project. This approach is analogous to having real-world monitoring data of the CO_2 and pressure plumes during the first 5 years of the injection period and using those monitoring results to assess the conformance of the predictions to real-world observations [4].

2. Methods

Burton-Kelly and others [5] provided details of the study methods; a summary is provided here. Fig. 1 shows the general workflow used in this study, which included the following primary components:

- **Generate a porosity volume:** Using publicly available data, a synthetic porosity volume was generated to emulate the complex subsurface geology at a higher resolution than is typical of data modeling workflows implemented as part of a storage project's routine site characterization. The porosity volume was representative of the type of product developed by acquiring 3D seismic data, performing a time-to-depth conversion, performing a poststack inversion (inverted compressional-wave velocity volume), and deriving a porosity volume from the inverted compressional-wave velocity volume.
- **Develop a standard reference geomodel:** A geomodel was developed within the porosity volume that was representative of the Broom Creek Formation near central North Dakota, a region of active interest for storage projects. This baseline geomodel, the SRG, was assumed to represent the real world and defined as the standard within which all facies and petrophysical properties were known exactly.
- **Generate synthetic well log curves from the SRG:** The SRG was sampled (drilled) to derive synthetic well logs that would emulate acquiring downhole measurements from boreholes as part of a storage project's routine site characterization phases.
- **Develop DGs from the SRG synthetic well logs:** The synthetic well logs and porosity volume acquired from the SRG were used to constrain the development of DG-Base, a geomodel that reflected the standard workflow of developing a geomodel for storage projects. It used synthetic well logs and porosity volume as the sole inputs. Two permutations of the DG-Base were developed using shorter (DG-Short) and longer (DG-Long) variogram lengths.

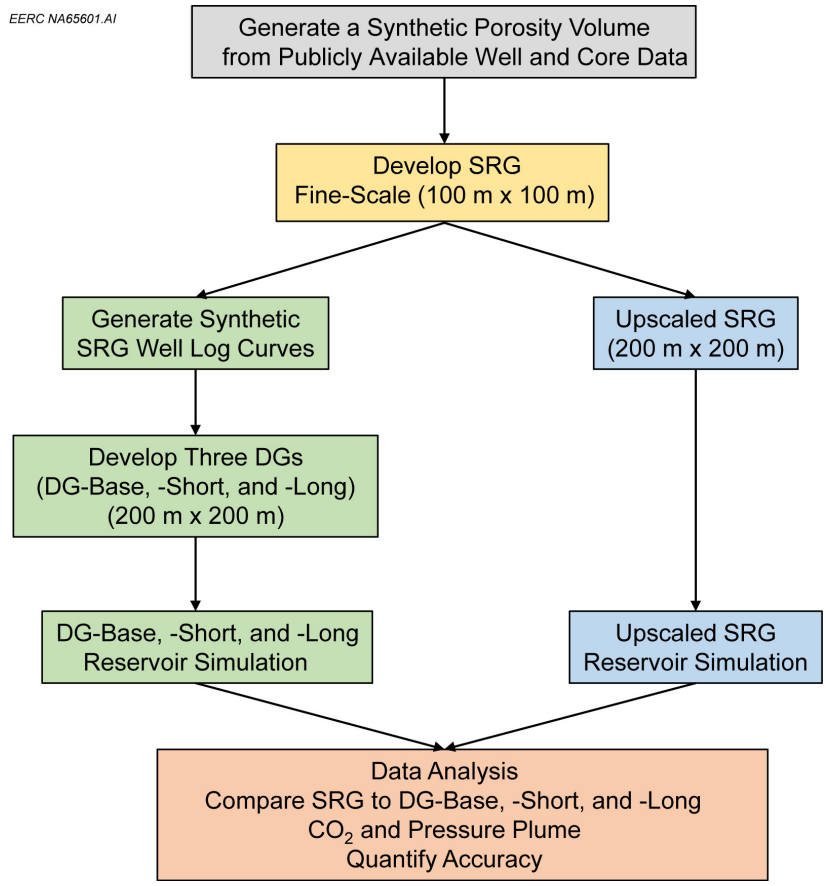

Fig. 1. Summary of the general workflow used in this study.

- **Conduct reservoir simulations:** Reservoir simulations of CO_2 injection for 5 years were performed in the SRG and the three DGs (DG-Base, DG-Short, and DG-Long). The monthly output (Months 1–60) of CO_2 saturation and pressure buildup within each storage unit geomodel grid cell was determined and recorded.
- **Perform data analysis and comparative assessment:** The facies and properties between the SRG and the DG-Base, DG-Short, and DG-Long geomodels were analyzed and compared along with the reservoir simulation results of CO_2 saturation (CO_2 plume) and pressure buildup within the storage unit.

2.1. Standard Reference Geomodel (SRG) Development

The geographic area investigated by this study was near central North Dakota, a region of active interest for storage projects. While the SRG was built to represent the Broom Creek Formation, it did not represent the actual subsurface at any given location. The SRG was developed using several public data sources containing geophysical well log data, core data results, and well files. Based on prior studies [6–8], the zone of interest (ZOI) was defined as the interval between the top of the Permian Opeche Formation, assumed to be the overlying confining formation (primary confining layer), and the base of the Pennsylvanian Amsden Formation, the underlying confining formation (lower confining layer), which included the complete Pennsylvanian Broom Creek Formation, considered as the injection zone or storage unit. *SRG structural modeling*: An 80 km × 80 km domain was defined as the SRG extent to contain the expected CO_2 plume and pressure buildup of the injection scenario over time. The top of the Broom Creek Formation was developed using a set of well depth correlations from a representative area of the Williston Basin. A trend surface was developed from the well correlations, and a Gaussian random function simulation was used to introduce more realistic variability (roughness) into each surface. The top of the Amsden Formation represented the

base of the storage unit and was developed using conformal gridding below the synthetic Broom Creek Formation surface with an isochore thickness derived from a representative area of the Williston Basin. The top and base of the modeled interval (defining the upper and lower confining zones, respectively) were calculated 100 m above and below the storage unit interval. The SRG had a grid of 100 m × 100 m cells. The confining zone was 50 cell layers, each 2 m thick (100 m total). The storage unit was 100 cell layers, and the layer thicknesses varied across the model area from 0.41 to 1.12 m, with a mean of 0.84 m. The SRG grid comprised 129 million cells, with 64 million cells in the storage unit. *SRG facies modeling*: Prior knowledge of the formation facies was initially used to generate the mineral phases incorporated into an object-based facies distribution within the SRG [9]. The SRG facies were determined by analyzing well log and core porosity, permeability, and rock composition using SLB Techlog 2022. The SRG was populated with six lithofacies (rock types): 1) dune sandstone, 2) interdune sandstone, 3) dolostone, 4) dolomitic sandstone, 5) anhydrite, and 6) confining lithologies. The object-modeling algorithm in Petrel was used to distribute facies in the SRG. *SRG porosity and permeability modeling*: Descriptive statistics for each facies were generated for the well log and core porosity analyses. The SRG porosity was modeled using the petrophysical modeling process in SLB Petrel 2021.5.0 to distribute porosity values by facies based on their descriptive statistics. Permeability was modeled using the Petrel calculator and regression models derived from regional core data to relate porosity to permeability within each facies.

2.1.1. SRG Grid and Property Upscaling

After the porosity and permeability were distributed in the fine-scaled SRG grid, the grid was upscaled from (SRG) 100 m × 100 m × 0.84 m cells to (upscaled SRG [USRG]) 200 m × 200 m × 2 m. Upscaling the grid resulted in a much lower cell count (8 million total cells with 6 million cells in the storage unit in the USRG versus 129 million total cells with 64 million cells in the storage unit in the SRG). The lower cell counts and the removal of null cells at the base of the storage unit were done to accelerate the simulation run times.

2.2. SRG Sampling

The SRG was sampled (drilled) to emulate a real-world site characterization and acquire information about the facies and petrophysical properties of the storage complex. Rather than use the exact SRG results at each grid cell, which would have been perfect knowledge of the facies and petrophysical properties, the workflow generated synthetic well logs to estimate porosity and permeability and better represent the type of imperfect knowledge inherent in subsurface site characterization. Five hypothetical wells were “drilled” into the SRG to derive synthetic well logs to emulate the real-world situation of acquiring downhole measurements from boreholes as part of a routine site characterization phase of a storage project. The five wells consisted of an injection well in the center of the SRG, surrounded by four observation wells, each located 9.05 km from the injection well—northeast, southeast, southwest, and northwest—forming a square with sides of 12.9 km. For each well, the SRG facies, porosity, and permeability were extracted from the SRG. Facies-specific regression models were used to produce functions for the wells and generate the typical curves commonly used in petrophysical analyses to characterize the ZOI. A Gaussian smoothing with a 1.5-m window was applied to the curves generated from the regression models. The synthetic smoothed logs for the five wells were used as inputs for the calculations performed in SLB Techlog 2022 to estimate the total porosity, volume of shale, effective porosity, and irreducible water saturation, which were then used in the Wyllie–Rose permeability calculation [10]. These properties were upscaled and used as input to the DGs.

2.3. Synthetic Porosity Volume Development

For situations where 3D seismic volumes can be inverted to porosity volumes, the seismic porosity inversion can assist in the development of an averaged representation of porosity at the seismic resolution both laterally and vertically. To test a simple synthetic seismic porosity inversion volume, a 6.4 km × 6.4 km submodel was extracted from the SRG storage unit and smoothed vertically and laterally using a combination of custom Petrel workflows and the Petrel property smoothing operations. The resulting synthetic seismic porosity volume was upscaled from the SRG to the DG-Base, and an experimental porosity variogram was calculated, incorporating the variability of the synthetic

seismic porosity for all facies together. This "global" variogram was used because the individual facies could not be distinguished at the resolution of the synthetic porosity inversion. Modified variogram models were calculated for the DG-Short and DG-Long models using the same major/minor ratio but with the long axis multiplied by 0.5 and 2, respectively.

2.4. Derivative Geomodel (DG) Development

Using the five synthetic well logs from the SRG, three DGs (DG-Base, DG-Long, and DG-Short) were built using representative industry-standard workflows to simulate possible outcomes for storage projects with limited site characterization data. All three DGs were built using the same workflow. *DG structural modeling*: The top (Broom Creek Formation top) and bottom (Amsden Formation top) of the storage unit were identified at the five wells. Petrel's convergent interpolation algorithm used the identified top and bottom to create structural surfaces. Grid cell size and layering were chosen to balance the amount of detail and simulation run time. The DGs were built using cells 200 m × 200 m, with different cell thicknesses for each zone. *DG facies modeling*: The five synthetic well logs were upscaled into the DG grid. The five reservoir facies identified in the SRG were distributed in the DG using sequential indicator simulation. Single facies were applied to the upper and lower confining zones. The global fraction and the fraction per layer of each facies in the storage unit were derived from the proportional statistics in the upscaled well logs using "fit vertical proportion curves" in Petrel's data analysis tool. The global variogram model used for each DG variation was taken from the upscaled synthetic seismic porosity volume. *DG porosity and permeability modeling*: The DG porosity and permeability were modeled using the petrophysical modeling process in Petrel to distribute porosity and permeability values by facies using Gaussian random function simulation. The porosity and permeability distributions for each facies were derived from the data from the five upscaled synthetic well logs. The global variogram model for each DG variation was taken from the upscaled synthetic seismic porosity volume.

2.5. Reservoir Simulation

Reservoir simulation evaluated the CO_2 and pressure responses in response to CO_2 injection into the SRG and the three DGs (DG-Base, DG-Short, and DG-Long). The reservoir simulation model was constructed using Computer Modelling Group Ltd.'s GEM. A 15 km × 15 km sector model was extracted from the full model extent. Reservoir simulation models were developed for the fine-scaled SRG, USRG, and the three upscaled DGs. The fine-scaled grid size was 100 m × 100 m × 0.84 m, and the upscaled grid size was 200 m × 200 m × 2 m. The fine-scaled reservoir simulation model included approximately 2 million grid cells, while the upscaled reservoir simulation model contained approximately 300,000 grid cells. Therefore, the simulation-case matrix focused on the upscaled model comparisons to accelerate the simulation run time.

CO_2 injection was simulated for 5 years. Different simulation cases were tested to compare the USRG to the three DGs. All simulations assumed the wellbore was perforated across the entire thickness of the storage unit. An initial simulation was conducted with the USRG using maximum bottomhole pressure (BHP) and wellhead pressure (WHP) constraints set to 27,579 kPa and 11,721 kPa, respectively, which were consistent with thresholds used by the EERC for similar reservoir simulations conducted for storage projects in this region of North Dakota (e.g., [9]). The simulation run with BHP/WHP constraints was used to identify the maximum CO_2 injection rate that could be sustained in the USRG without exceeding the BHP and/or WHP constraints, which was 0.81 million tonnes CO_2/year (3000 m^3 CO_2/day). The subsequent simulations with the DGs applied this injection rate constraint to create comparable cases of the USRG and DG simulations for evaluating the CO_2 and pressure plume behaviors. Four simulations were included in the injection rate-constrained case matrix: Case 1 (USRG), Case 2 (DG-Base), Case 3 (DG-Short), and Case 4 (DG-Long).

2.6. Data Analysis and Comparative Assessment

The data analysis aimed to quantitatively compare the simulated CO_2 and pressure plumes in the storage unit between the USRG and three DGs (DG-Base, DG-Short, and DG-Long). The 3D CO_2 and pressure plumes in the

storage unit were translated to 2D grids for Months 1–60 of CO_2 injection. These 2D grids were created by projecting the multiple geologic model layers of the 3D storage unit onto a 2D grid, which presented the CO_2 and pressure plume extents in map view. For the CO_2 plume, the maximum CO_2 saturation in the 3D model (represented by x, y, and z) was extracted from the vertical z dimension and assigned to each cell of the 2D grid [11]. Similarly, for the pressure plume, the maximum value of pressure buildup in the 3D model (represented by x, y, and z) was extracted from the vertical z dimension and assigned to each cell of the 2D grid. The outputs from this translation were sets of 2D grids for the CO_2 and pressure plumes for the USRG, DG-Base, DG-Short, and DG-Long simulations. All subsequent calculations were applied to the 2D grids. The CO_2 and pressure plumes were translated from continuous to binary values. Individual grid cells in the 2D grids were either outside (value = 0) or inside (value = 1) of the CO_2 or pressure plume. The CO_2 plume extent was defined as ≥5% CO_2 saturation [12–15]. The pressure plume extent was defined as a change in pressure ≥100 kPa. The outputs from this binary process were sets of grids with cell values equal to either 0 (beyond the CO_2 or pressure plume extent) or 1 (within the CO_2 or pressure buildup extent) for the USRG, DG-Base, DG-Short, and DG-Long simulations. The 2D binary grids from the preceding step were used to calculate the number of concordant pairs (i.e., the number of grid cells where the USRG and DG agree) and the number of discordant pairs (i.e., the number of grid cells where the USRG and DG disagree). This binary comparison had four possible outcomes:

A. USRG = DG = 1 (concordant, both the USRG and the DG predict CO_2 saturation ≥5% in the same grid cell).
B. USRG = 0 but DG = 1 (discordant, the USRG predicts CO_2 saturation <5%, but the DG predicts CO_2 saturation ≥5% in the same grid cell).
C. USRG = 1 but DG = 0 (discordant, the USRG predicts CO_2 saturation ≥5%, but the DG predicts CO_2 saturation <5% in the same grid cell).
D. USRG = DG = 0 (concordant, both the USRG and the DG predict CO_2 saturation <5% in the same grid cell).

The four possible outcomes for the pressure plumes were the same, but the 100-kPa threshold was used to denote 0s and 1s. The four outcomes were organized in a confusion matrix to calculate accuracy measures. The current study used four accuracy measures: (1) simple matching coefficient (SMC), (2) Rogers and Tanimoto coefficient (RTC), (3) Legendre and Legendre coefficient (LLC), and (4) Jaccard similarity coefficient (JSC). The SMC is a similarity coefficient that considers the presence or absence of the data to calculate the similarity between two grids [16]. An SMC of 1 is a perfect concordance, and an SMC of 0 is a perfect discordance. Since the SMC considers both presence (1) and absence (0), it is a symmetrical coefficient. In early simulation times, when most grid cells are 0 because of the absence of a CO_2 or pressure plume, the SMC will be artificially inflated toward perfect concordance (i.e., closer to 1). The RTC is a variant of the SMC that emphasizes discordance (i.e., outcomes B and C) [17]. The LLC is another variant of the SMC that places more emphasis on concordance (i.e., outcomes A and D). The LLC considers the presence or absence of data and calculates the similarity between two matrices [18]. Lastly, the JSC is like the SMC, but concordance represented by joint absences (outcome D) does not contribute toward the similarity. Therefore, the JSC is an asymmetrical coefficient [19].

3. Results

Evaluations of the fine-scaled SRG, USRG, and three DGs (DG-Base, DG-Short, and DG-Long) showed differences in the facies, porosity, and permeability distributions, attributable to the information loss in going from the fine-scaled SRG to the synthetic well logs for the five wells “drilled” into the SRG, development of the DG-Base model from the five synthetic logs, and upscaling. In addition, the variogram changes to create the DG-Short and DG-Long models impacted the spatial trends in facies, porosity, and permeability, with the DG-Long resulting in more continuous distributions than the DG-Base (longer continuous regions of grid cells of similar values) and the DG-Short resulting in more variable distributions than the DG-Base (shorter continuous regions of grid cells of similar values). Burton-Kelly and others (2024) provided extensive results comparing the geomodels, simulations, and accuracy measures. Select results are provided here to compare the USRG and DG simulations.

3.1. Reservoir Simulation Comparisons

This section describes four sets of simulation outputs. Each subsection visually compares outputs by providing vertical "slices" of the simulations in the x–z plane (east to west) or y–z plane (north to south) to show profiles of the geomodel grids and the spatial distribution of the simulated CO_2 saturation (CO_2 plume) or pressure buildup within the simulation model.

3.1.1. USRG Versus DG-Base CO_2 and Pressure plumes

Fig. 2 compares the CO_2 saturation at the end of 5 years in the USRG and DG-Base. In both models, the CO_2 plume was concentrated in the upper section of the storage unit, where a high-permeable zone was located. The lateral extents of the CO_2 plumes in the X-Z plane (east to west) were comparable. However, as shown in the figure, the DG-Base simulation extended slightly further to the east than the USRG simulation and slightly less than the USRG to the west. The lateral extents of the CO_2 plumes in the Y–Z plane (north to south) were similar. These differences were attributable to the differences in facies, porosity, and permeability, which affected the reservoir simulations of fluid flow within the storage unit. Fig. 3 compares the pressure buildup at the end of 5 years in the USRG and DG-Base. The zones of greatest pressure buildup in the near-wellbore region, indicated in red in the figure, differed between the USRG and the DG-Base. This result was attributable to the permeability distribution around the injection well, which was a function of the facies and porosity distributions for the USRG and DG-Base. The USRG contained two lower-permeability regions near the wellbore, which were not present to the same degree in the DG-Base. Consequently, the two dark red zones observed in the USRG were not observed in the DG-Base. The lateral extents of the pressure plumes also differed.

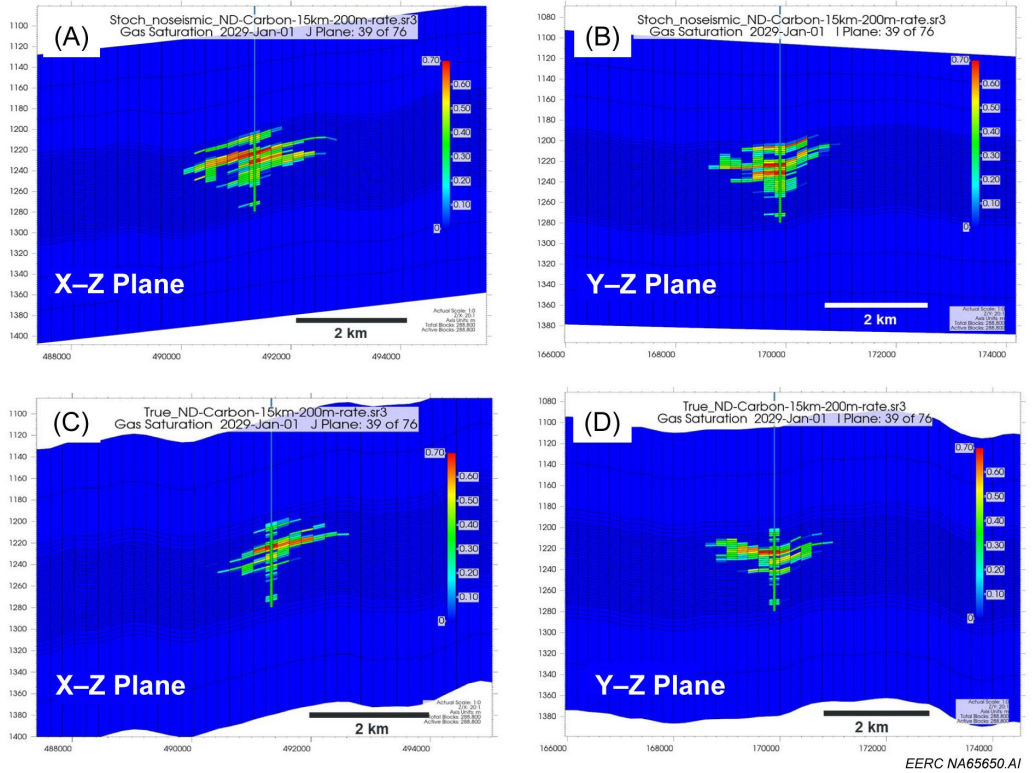

Fig. 2. CO_2 saturation in the storage unit (fraction) after 5 years of CO_2 injection in the injection rate-constrained DG-Base simulation (Case 2: top row, A and B) and the injection rate-constrained USRG simulation (Case 1: bottom row, C and D) showing the J=39 layer (x–z plane, left) and the I=39 layer (y–z plane, right).

3.1.2. DG-Short Versus DG-Long CO_2 and Pressure plumes

The DG-Short and DG-Long models were developed with shorter and longer variogram lengths. Therefore, the spatial distribution of rock facies, porosity, and permeability were shorter or more heterogeneous/discontinuous in the DG-Short and longer or more homogeneous/continuous in the DG-Long. The shortening and lengthening of the spatial distributions of rock facies, porosity, and permeability affected the behavior of the CO_2 plumes. For example, even though the same rates of CO_2 were injected into both models (3000 m^3 CO_2/day), the CO_2 plume migrated laterally longer in the DG-Long than in the DG-Short. This extended migration of the CO_2 plume was caused by more continuous property distributions in the DG-Long model. However, in the DG-Short model, the CO_2 plume propagation was shorter and primarily near the injection well because the reservoir properties with short variogram lengths were discontinuously distributed in the storage unit. Similarly, the different property distributions also affected the pressure buildup responses, with significantly greater pressure buildup near the injection well in DG-Short than in DG-Long despite identical injection rates for both simulations.

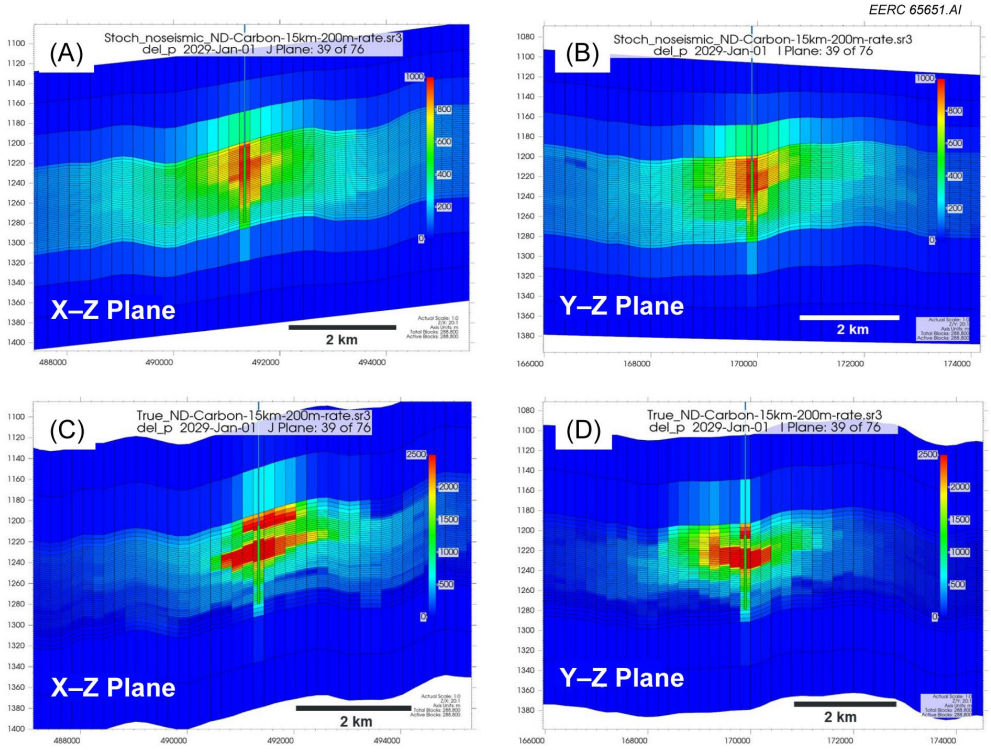

Fig. 3. Pressure buildup in the storage unit (kPa) after 5 years of CO_2 injection in the injection rate-constrained DG-Base simulation (Case 2: top row, A and B) and the injection rate-constrained USRG simulation (Case 1: bottom row, C and D) showing the J=39 layer (x–z plane, left) and the I=39 layer (y–z plane, right).

3.2. Accuracy Measures

The accuracy measures were evaluated for Months 1–60 (5 years) to assess how the USRG-simulated CO_2 and pressure plumes compared to those of the DG-Base, DG-Short, and DG-Long simulations. Depending on the specific measure, at the end of 60 months, the similarity ranged from 0.71 (JSC) to 0.91 (LLC) for the USRG versus the DG-Base. Joint absences do not contribute toward the JSC, whereas the LLC places more emphasis on joint presence (where the values of cells in the USRG and the DG grids equal 1) and joint absence (where the USRG and the DG grids are both 0). Since at the end of 60 months 130 of the 240 USRG grid cells did not contain CO_2, the SMC, RTC,

and LLC were closer to 1 than the JSC because the joint 0s contributed to all similarity measures except the latter. The DG-Short and DG-Long variations of the DG-Base had comparable similarity measures; however, the DG-Short was consistently lower (less like the USRG), while the DG-Long was consistently higher (more like the USRG) than the DG-Base at the end of 60 months. The similarity measures indicated that the DG-Long model was the most appropriate for estimating the spatial distribution of the CO_2 plume, particularly after 40 months, as its similarity metrics were greatest and, therefore, closest to the USRG.

The time-series progressions of the four similarity measures for the pressure plumes were like the trends for the CO_2 plumes. As expected, the pressure plumes were much larger than the CO_2 plumes. For example, at the end of 60 months, the CO_2 plume for the USRG was 4.4 km^2 (110 of 240 grid cells with ≥5% CO_2 saturation), whereas the pressure plume was 48.8 km^2 (1217 of 1813 grid cells with pressure buildup above 100 kPa).The pressure plume comparisons may have been affected by these differences in area and the effects of projecting the maximum pressure buildup in each x–y map-view grid cell anywhere in the z domain onto the 2D grid.

3.2.1. Discordance for the CO_2 Plume

The similarity metrics aggregated information across the entire 2D grid. For example, 240 grid cells were within the CO_2 plume at the end of 5 years in the USRG; however, 900 grid cells were in the full evaluation extent. Consequently, the proportion of grid cells with concordance for CO_2 and concordance for no CO_2 could have masked one of the fundamental aims of the study: understanding discordance for CO_2 where either the USRG and DG did not agree (outcome B: USRG = 0 but DG = 1, or outcome C: USRG = 1 but DG = 0). Although the RTC emphasizes discordance (outcomes B and C) and joint absences (outcome D) do not contribute toward the JSC, additional work was done to evaluate only the discordance outcomes of the simulated CO_2 plume.

Fig. 4 shows discordance maps that compare outcomes B and C between the USRG (Case 1) and the DG-Base (Case 2), DG-Short (Case 3), and DG-Long (Case 4) simulation results at the end of 5 years using the injection rate-constrained cases. The left column in Fig. 4 shows outcome B, where the USRG simulation predicted no CO_2 in a grid cell (USRG = 1), but the DG simulation predicted CO_2 in that grid cell (DG = 0). The CO_2 plume predicted from the USRG simulations is shown in blue cells, and the type-B discordance is shown in yellow cells. Across all three DGs, there was discordance in the northwest area of the CO_2 plume, where the DG simulations predicted CO_2 but the USRG simulation did not. The DG-Long simulation also predicted CO_2 in the eastern, southeastern, and southern areas of the CO_2 plume, whereas the USRG simulation did not. The geomodel grid cells for the USRG and all three DGs were 200 m × 200 m; therefore, the maximum distance for a type-B discordance was 600 m (three grid cells) for the DG-Base. However, most type-B discordances were one grid cell and, therefore, 200 m.

The right column of Fig. 4 shows outcome C, where the USRG simulation predicted CO_2 in a grid cell, but the DG simulation predicted no CO_2 in that grid cell. The type-C discordance is shown in red. The DG-Base and DG-Short simulations underpredicted the CO_2 plume along the southwestern, southeastern, eastern, northeastern, and northern areas. The DG-Long simulations had fewer discordances, with several mismatches in the southwestern and northern areas of the CO_2 plume. The maximum distance for a type-C discordance was 800 m (four grid cells) for the DG-Base simulation. However, most of the type-C discordances were one or two grid cells and, therefore, 400 m or less.

Additional testing would need to be conducted to assess the accuracies more definitively between the USRG and DG simulations, including simulations that included different injection rates, different reservoir properties, and the stabilized CO_2 plume after injection ceases (e.g., 20 years of injection plus at least 10 years of postinjection until the CO_2 plume was stabilized). However, based on these results for the first 5 years of injection, the DG simulations (the geomodels constructed using an industry-standard workflow and thus representative of models that would be generated from real-world data for commercial storage projects) were able to predict the 5-year CO_2 plume in the "real world" (as defined by the USRG simulations) to within 200–800 m. The DGs overpredicted the CO_2 plume in some areas (e.g., type-B discordances in the northwestern area) and underpredicted the CO_2 plume in other areas (e.g., type-C discordances along the southwestern, southeastern, eastern, northeastern, and northern areas). These results suggest a reasonable level of accuracy, especially considering that the predicted CO_2 plumes will be reevaluated at least every 5 years under the Class VI Rule, at which time the reservoir simulations would be recalibrated (history-matched) to the available field data and new forecasts would be generated.

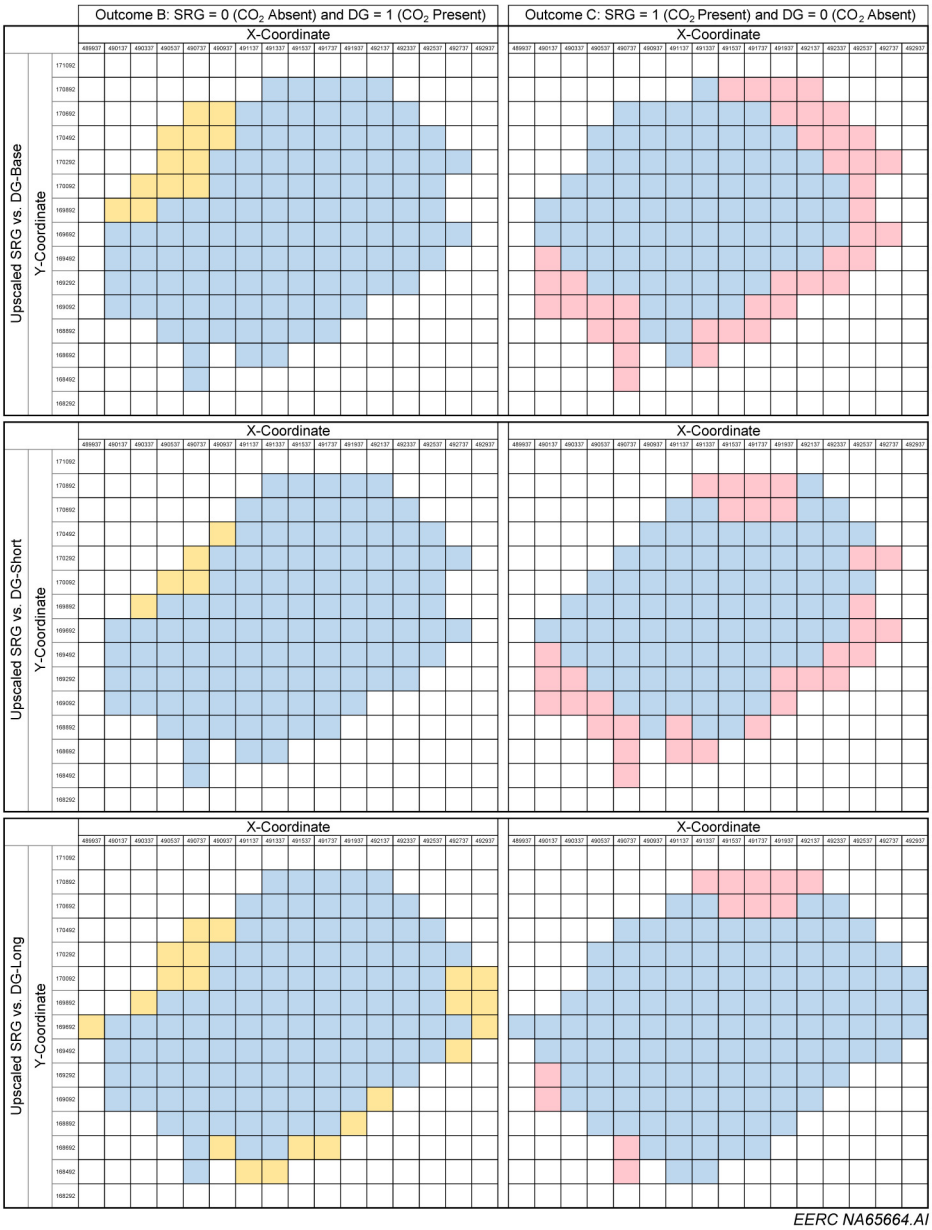

Fig. 4. Discordance outcomes for comparisons between the USRG and DG-Base (top row), DG-Short (middle row), and DG-Long (bottom row) for the simulated CO_2 plume at the end of 5 years using the injection rate-constrained cases. The left column shows outcome B, where the USRG simulation predicted no CO_2 in a grid cell, but the DG simulation predicted CO_2 in that grid cell. Type-B discordance is shown in yellow. The right column shows outcome C, where the USRG simulation predicted CO_2 in a grid cell, but the DG simulation predicted no CO_2 in that grid cell. Type-C discordance is shown in red. The blue grid cells show where the USRG and DGs agree (concordance).

4. Conclusions

This study estimated the accuracy of the predicted 5-year CO_2 and pressure plumes for a hypothetical storage project injecting CO_2 into the Broom Creek Formation near central North Dakota. The workflow defined an SRG for the Broom Creek Formation near central North Dakota, sampled the SRG at five well locations, and used synthetic logs acquired from these five wells to create one base-case DG, named DG-Base, and two permutations of the base

case developed with shorter and longer variogram lengths, DG-Short and DG-Long, respectively. The model-building process used to develop the DGs followed an industry-standard workflow; thus, the three DGs reflect the models generated from data acquired for a commercial storage project. Reservoir simulations were conducted in each geomodel, and the 5-year simulated CO_2 and pressure plumes in the storage unit were compared between the SRG and the three DGs using visual assessments and an array of accuracy metrics. The SRG-simulated results were defined as the true outcome (i.e., perfect knowledge of the future) and served as a basis for evaluating how well the reservoir simulation predictions generated in the DGs compared to the known future (conformance) [4]. The results showed the impacts of multiple elements of the geomodeling and reservoir simulation processes on the comparability between the SRG and the DGs. Key observations include:

- The sampling of the SRG to inform the facies, porosity, and permeability of the DGs significantly affected the simulation results. The SRG sampling at five well locations utilized regression models and Gaussian smoothing to generate synthetic (rebuilt) logs to avoid biasing the well logs with perfect information on the SRG properties. The information loss resulted in rebuilt well logs with slightly less heterogeneity in porosity and permeability than the SRG well logs. However, information loss between the SRG and downhole geophysical measurements acquired through well logs may represent a similar type of error that could be introduced at an actual storage site. Additional research is needed into how the geomodel is affected by the degree of information loss (i.e., the agreement between the true well log and the rebuilt well log) and the number of wells included in the sampling and geomodel-building (beyond the five-well example used in the current study).
- The processes used to distribute facies, porosity, and permeability, including upscaling to large grid sizes, within the DGs had a significant effect. The variogram model used for DG-Base, DG-Short, and DG-Long was derived from an imperfect aggregate sample of the SRG porosity (the synthetic seismic porosity inversion volume) rather than separate (in practice, unknowable) representative samples of the variogram for each facies. In general, the physical continuity of the most porous rock was underestimated in DG-Base and DG-Short, resulting in smaller plumes than the USRG. It was overestimated in DG-Long, resulting in larger plumes. Additional research is needed on how the geomodel is affected by the variogram settings (azimuth, major range, minor range, vertical range, and/or structure).
- The reservoir simulation constraints, which included BHP/WHP and/or injection rate constraints, significantly affected the injection rates and, therefore, the cumulative mass of CO_2 injected into the different geomodels. These outcomes were impacted by the upscaling from a 100-m, fine-scaled SRG to the 200-m, upscaled SRG and DGs. By upscaling the grid size, the total number of grids was reduced from 2 million grid cells to 300,000 grid cells, and the simulation time was reduced from 12 hours for the fine-scaled SRG model to 20 minutes for the USRG model—a computational cost savings of approximately 97%. However, these gains in computational efficiency came at the cost of grid cell properties and injectivity. To reduce these errors, smaller grid sizing and improving computational tools (e.g., more advanced computers or cloud computing) may be necessary.

A novel application of similarity metrics within a 2D grid was used to assess the accuracy between the USRG and DG simulations. Despite the sources of uncertainty in the geomodels and reservoirs simulations, the comparative assessments showed that the DG simulations could predict the 5-year CO_2 plume at a storage site (as defined by the USRG simulations) to within 200–800 m. The DGs overpredicted the CO_2 plume in some areas and underpredicted the CO_2 plume in others. Additional testing could assess these accuracies more definitively and validate these preliminary findings.

Like any model, constructing a geomodel for a storage project simplifies the surface and subsurface environments to provide a tractable tool for answering relevant questions about the future behavior of CO_2 and pressure in the storage unit in response to CO_2 injection. Throughout the geomodel-building process, aspects of the sampling done to facies, porosity, and permeability affect the final geomodel. In addition, processes used to distribute facies, porosity, and permeability, including upscaling to larger grid sizes, also affect the final geomodel. Overlaid onto these sources of uncertainty in the geomodel are the uncertain inputs and settings for the reservoir simulations. These additional uncertainties also impact the simulations of CO_2 and pressure propagation within the geomodel. The workflow used in this study was not an exhaustive search of all possible uncertain input parameters in the geomodeling and reservoir simulation workflows. However, the SRG development, SRG sampling, DG development, reservoir simulations, and

comparative assessments provide a template for future research to improve uncertainty quantification in CO_2 and pressure plume predictions.

Acknowledgments

This material is based upon work supported by the U.S. Department of Energy National Energy Technology Laboratory under Award Numbers DE-FE0031889 and DE-FE0031838.

References

[1] Sorensen, J.A., Bailey, T.P., Dobroskok, A.A., Gorecki, C.D., Smith, S.A., Fisher, D.W., Peck, W.D., Steadman, E.N., and Harju, J.A., 2009, Characterization and modeling of the Broom Creek Formation for potential storage of CO_2 from coal-fired power plants in North Dakota: Search and Discovery Article #80046.

[2] Peck, W.D., Glazewski, K.A., Braunberger, J.R., Grove, M.M., Bailey, T.P., Bremer, J.M., Gorz, A.J., Sorensen, J.A., Gorecki, C.D., and Steadman, E.N., 2014, Broom Creek Formation outline: Plains CO_2 Reduction (PCOR) Partnership Phase III value-added report for U.S. Department of Energy National Energy Technology Laboratory Cooperative Agreement No. DE-FC26-05NT42592, EERC Publication 2014-EERC-09-09, Grand Forks, North Dakota, Energy & Environmental Research Center.

[3] Department of Mineral Resources, 2024, Class VI—geologic sequestration wells: www.dmr.nd.gov/dmr/oilgas/ClassVI (accessed January 2024).

[4] Oldenburg, C.M., 2018, Are we all in concordance with the meaning of the word conformance, and is our definition in conformity with standard definitions?: Greenhouse Gases: Science and Technology, v. 8, p. 210–214. DOI: 10.1002/ghg.1773

[5] Burton-Kelly, M.E., Martinez, G.A., Min, K., Chakhmakhchev, A., Belobraydic, M.L., Azzolina, N.A., Nakles, D.V., and Peck, W.D., 2024, A quantitative assessment of the simulated CO_2 and pressure buildup plume accuracy for a hypothetical CO_2 storage project in central North Dakota, North Dakota CarbonSAFE Phase III Topical Report, June 2024.

[6] Bosshart, N.W., Azzolina, N.A., Ayash, S.C., Peck, W.D., Gorecki, C.D., Ge, J., Jiang, T., and Dotzenrod, N.W., 2018, Quantifying the effects of depositional environment on deep saline formation CO_2 storage efficiency and rate: International Journal of Greenhouse Gas Control, v. 69, p. 8–19.

[7] Burton-Kelly, M.E., Azzolina, N.A., Connors, K.C., Peck, W.D., Nakles, D.V., and Jiang, T., 2021, Risk-based area of review estimation in overpressured reservoirs to support injection well storage facility permit requirements for CO_2 storage projects: Greenhouse Gas Science and Technology, v. 11, p. 887–906.

[8] Peck, W.D., Ayash, S.C., Klapperich, R.J., and Gorecki, C.D., 2019, The North Dakota integrated carbon storage complex feasibility study: International Journal of Greenhouse Gas Control, v. 84, p. 47–53.

[9] Peck, W.D., Azzolina, N.A., Nakles, D.V., Glazewski, K.A., Klapperich, R.J., Crocker, C. R., Oster, B.S., Daly, D.D., Livers-Douglas, A.J., Butler, S.K., Smith, S.A., Botnen, B.W., Feole, I. K., He, J., Dotzenrod, N.D., Salazar, A.Y., Patil, S.B., and Crossland, J.L., 2020, North Dakota integrated carbon storage complex feasibility study: Final report for the period June 9, 2017 – February 8, 2020. University of North Dakota Energy & Environmental Research Center, 285 p.

[10] Wyllie, M.R.J., and Rose, W.D., 1950, Theoretical considerations related to quantitative evaluation of physical characteristics of reservoir rocks from electrical log data: Transactions of the AIME, v. 189, p. 105–118.

[11] Regorrah, J.G., Hunt, J.E., Templeton, J.A., Dotzenrod, N.W., Azzolina, N.A., Dalkhaa, C., Peck, W.D., Livers-Douglas, A.J., and Connors, K.C., 2023, A quantitative approach for demonstrating plume stabilization under CCS policy frameworks: EERC Publication 2023-EERC-05-02, Grand Forks, North Dakota, Energy & Environmental Research Center.

[12] Whittaker, S., White, D., Law, D., and Chalaturnyk, R., 2004, IEA GHG Weyburn CO_2 monitoring and storage project summary report, 2000–2004, *in* Wilson, M., and Monea, M. [eds.], Proceedings of the 7th International Conference on Greenhouse Gas Control Technologies: September 5–9, 2004, Vancouver, Canada, Volume III.

[13] White, D.J., Roach, L.A.N., Roberts, B., and Daley, T.M., 2014, Initial results from seismic monitoring at the Aquistore CO_2 storage site, Saskatchewan, Canada: Energy Procedia, v. 63, p. 4418–4428. DOI: 0.1016/j.egypro.2014.11.477.

[14] Roach, L.A.N., White, D.J., and Roberts, B., 2014, Assessment of 4D seismic repeatability and CO_2 detection limits using a sparse land array at the Aquistore CO_2 storage site: Geophysics, v. 80, p. WA1-WA13. DOI: 0.1190/GEO2014-0201.1.

[15] Roach, L.A.N., White, D.J., Roberts, B., and Angus, D., 2017, Initial 4D seismic results after CO_2 injection start-up at the Aquistore storage site: Geophysics, v. 82, B95-B107. DOI: 10.1190/geo2016-0488.1.

[16] Sokal, R.R., and Michener, C.D., 1958, A statistical method for evaluating systematic relationships: University of Kansas Scientific Bulletin, v. 38, p. 1409–1438.

[17] Rogers, D.J., and Tanimoto, T.T., 1960, A computer program for classifying plants: Science, v. 132, p. 1115–1118. DOI: 10.1126/science.132.3434.1115.

[18] Legendre, P. and Legendre, L., 1998, Numerical ecology (2d English ed.): Amsterdam, Elsevier, 853 p.

[19] Jaccard, P., 1901, Étude comparative de la distribution florale dans une portion des Alpes et des Jura: Bulletin de la Société Vaudoise des Sciences Naturelles, v. 7, p. 547–579.